Check for updates

Received: 25 January 2025 | Accepted: 6 February 2025

DOI: 10.1002/ecs2.70326

ECOSPHERE
AN ESA OPEN ACCESS JOURNAL

ARTICLE

Coastal and Marine Ecology

Spatially dynamic abundance patterns for a rare fish species

Valerie A. Steen[1] | **James T. Peterson**[2] | **Adam Duarte**[3]

[1]Oregon Cooperative Fish and Wildlife Research Unit, Department of Fisheries, Wildlife, and Conservation Sciences, Oregon State University, Corvallis, Oregon, USA

[2]U.S. Geological Survey, Oregon Cooperative Fish and Wildlife Research Unit, Department of Fisheries, Wildlife, and Conservation Sciences, Oregon State University, Corvallis, Oregon, USA

[3]U.S.D.A. Forest Service, Pacific Northwest Research Station, Olympia, Washington, USA

Correspondence
Valerie A. Steen
Email: valerie.steen@gmail.com

Present address
Valerie A. Steen, CEMML, Colorado State University, Fort Collins, Colorado, USA.

Funding information
Metropolitan Water District of Southern California, Grant/Award Number: 187386

Handling Editor: Sean P. Powers

Abstract

Recovery of rare and imperiled species is often supported by targeting the dynamic drivers of abundance patterns. However, knowledge of these drivers can be obscured by challenges stemming from species detectability and autocorrelated data. Longfin Smelt (*Spirinchus thaleichthys*) in the San Francisco Bay-Delta have become rare as the result of dramatic declines in abundance. Abundance indices from a multitude of surveys in the Bay-Delta have documented these declines, but utilizing survey data to support recovery has been more challenging. To elucidate the spatiotemporal drivers of Longfin Smelt abundance patterns, we employed spatial multistate ("abundant") dynamic occupancy models that integrated surveys across seasons from three fish monitoring programs. We found that species occupancy may be driven by broad-scale temporal and spatial processes not accounted for in the environmental covariates we used given the relative importance of day of year and spatial and year random effects. However, we also found that relatively high abundance may be driven in part by local habitat conditions. Our analysis approach allowed us to capture various sources of heterogeneity in the data and map seasonal distribution and abundance patterns for this rare species that can be used to inform policy and management decisions in the Bay-Delta.

KEYWORDS
integrated modeling, Longfin Smelt, monitoring, San Francisco Bay-Delta, spatial dynamic multistate occupancy models, *Spirinchus thaleichthys*

INTRODUCTION

Elucidating drivers of species distributions is critical to inform species management and can make the difference between recovery and extinction (Bain et al., 2007; Coonan et al., 2010; Guisan & Thuiller, 2005; Solomon, 1998). While distributions of fish and wildlife are often treated as static, animals move, are recruited into the population, and die, resulting in dynamic distribution patterns owing to these dynamic processes (Guillera-Arroita, 2017; Kéry et al., 2013). Therefore, the drivers of species distributions may depend on life stage or time of year. Understanding these complex patterns may be key to effective management, such as targeting limiting factors present during certain life stages, or to form multifaceted management plans with elements for the full annual cycle (e.g., de Paula Costa et al., 2022; Rosenberg et al., 2016).

Insights into distribution patterns benefit from statistical approaches that account for all important phenomena giving rise to these patterns (reviewed in Kéry & Royle, 2016). While environmental drivers are typically

This is an open access article under the terms of the Creative Commons Attribution License, which permits use, distribution and reproduction in any medium, provided the original work is properly cited.
© 2025 The Author(s). *Ecosphere* published by Wiley Periodicals LLC on behalf of The Ecological Society of America.

of interest, imperfect detection of animals and unexplained variation are also important features of statistically based models of species distributions (MacKenzie et al., 2017). Imperfect detectability may result in undercounting individuals. Additionally, it can confound environmental relationships when detection itself is related to an environmental feature (Gu & Swihart, 2004; Tyre et al., 2003). For example, it would be difficult to assess how streamflow affects resident fish populations without addressing that fish are more difficult to catch when water is deep and currents are swift (Peterson & Paukert, 2009). Unexplained variation in distribution patterns that cannot be accounted for by the known or available environmental drivers is also important to model (Dormann, 2007; Hurlbert, 1984). An estimate of this *spatial autocorrelation* assesses the amount of variation in distribution patterns that remains unexplained. If a large amount of variation is unexplained, it can be a prompt to search for the missing information, perhaps an important environmental driver (Dormann et al., 2007). It also reduces the likelihood of type I error, falsely concluding a variable is significant (Dormann et al., 2007).

Rare and imperiled species are paradoxically the most in need of statistically sound insights and are also often data limited for these data-dependent methods (Jeliazkov et al., 2022; Lomba et al., 2010). This has led to the popularity of occupancy models for modeling rare species (Durso et al., 2011; Linkie et al., 2007; Specht et al., 2017). Occupancy models are an important class of species distribution models that estimate true occupancy by explicitly accounting for imperfect detection (MacKenzie et al., 2003). While they require repeat surveys, the model assumptions are generally reasonably met for most studies (reviewed in Kéry & Royle, 2016). The Bernoulli error distribution used to estimate occupancy probability inherently works with data with a large proportion of zeros, the type of data rare species tend to produce. Additionally, dynamic processes can be explicitly modeled to describe and understand changing occupancy of sites (MacKenzie et al., 2009).

While occupancy models have significant advantages, they reduce any information on variation in abundance to 1 or 0, detected or not detected. Multistate occupancy models—a type of occupancy model with more than two states—can bridge this gap by estimating different abundance states, for example, low abundance versus high abundance (MacKenzie et al., 2009). Furthermore, multistate occupancy models retain the advantages of the basic occupancy model by having reasonable assumptions, separating the process giving rise to the zeros in the data, and the ability to model dynamic occupancy. While they have seen limited use for modeling abundance patterns of rare species, a recent simulation paper verified their efficacy for this purpose (Steen et al., 2023).

The fish of the San Francisco Bay-Delta (hereafter Bay-Delta) serve as a useful case study for testing the value of advanced empirical approaches for improving insights to support rare fish species management. Many historically abundant native fish species in the Bay-Delta have declined to low numbers such that they have become rare and in need of management intervention to avoid becoming extirpated (Newman, 2008; Sommer et al., 2007; Sweetnam & Stevens, 1993). Implicated causes include many of the usual challenges for aquatic systems worldwide, such as flow alterations and water diversion, introduced species, and climatic shifts (Herbold et al., 2022; Kimmerer, 2008; Kimmerer & Orsi, 1996; Nobriga & Rosenfield, 2016; Sommer et al., 2007). In the Bay-Delta, fish are sampled regularly (biweekly to monthly) by a multitude of surveys to document population changes and inform management strategies to support species recovery (Stompe et al., 2020). Annual population indices using mean fish counts across surveys have documented precipitous population declines for numerous species (Newman, 2008; Sweetnam & Stevens, 1993). They have historically been the basis for management (e.g., Sommer et al., 2007; Stompe et al., 2020; Thomson et al., 2010) enabling research into the response of fish to key environmental variables in the Bay-Delta including turbidity (measured as secchi depth), temperature, and salinity, along with estimated daily Delta outflows from the Sacramento and San Joaquin rivers and the related "X2" line—the distance from the Golden Gate Bridge to the point where the salinity is 2 parts per thousand at a depth of 1 m below the surface (e.g., Hammock et al., 2019; Mac Nally et al., 2010; Peterson & Barajas, 2018). Importantly, these surveys also pointed to a knowledge gap: Peterson and Barajas (2018) found a strong spatial signal in fish distributions—quantified as spatial random effects—that was not accounted for by these environmental variables. The large spatial effect indicated that specific locations were persistently more or less occupied than others, indicating a large gap in understanding of the spatial drivers of fish distributions in the Bay-Delta. These indices are now regarded as limited for informing species recovery, given biases from imperfect detectability and the need to understand spatially dynamic distributions of these highly mobile species (Duarte & Peterson, 2021; Latour, 2016; Mahardja et al., 2017; Mitchell et al., 2017, 2019; Newman, 2008; Peterson & Barajas, 2018; Polansky et al., 2018; Simonis & Merz, 2019).

Spatial dynamic multistate occupancy models explicitly address imperfect detection and spatial autocorrelation, and multiple states can be defined to estimate

21508925, 2025, 7, Downloaded from https://esajournals.onlinelibrary.wiley.com/doi/10.1002/ecs2.70326, Wiley Online Library on [14/07/2025]. See the Terms and Conditions (https://onlinelibrary.wiley.com/terms-and-conditions) on Wiley Online Library for rules of use; OA articles are governed by the applicable Creative Commons License

variation in abundance. We focused on the Bay-Delta Longfin Smelt (*Spirinchus thaleichthys*), a fish that moves between the freshwater delta, brackish bay, and nearshore coastal areas depending on life stage. Our objectives were twofold: (1) to develop a more cohesive understanding of the distribution and abundance patterns of the Bay-Delta Longfin Smelt to support recovery for this federally endangered population and (2) to elucidate a framework for modeling distributions of rare species. In the multistate occupancy model, we defined three categories of site-level abundance: not-occupied, occupied (but *not* relatively abundant), and relatively abundant states to estimate abundance dynamics while accounting for imperfect detection and spatial autocorrelation. Given the availability of different surveys conducted during different seasons but at a consistent set of 30 stations (hereafter *site*), we created an integrated model by estimating detectability for each dataset but estimating dynamic occupancy together. By integrating datasets into a single spatial dynamic multistate occupancy model, we provide a more tenable accounting for the species' known variability in detectability, distribution, and abundance patterns while also increasing the temporal resolution of population dynamics by modeling the spatial and temporal autocorrelation inherent in the count data.

METHODS

Study area

The San Francisco Bay-Delta is formed of the San Francisco Bay and, to the northeast, a large inland delta made up of the confluence of the 111,000 km^2 Sacramento and San Joaquin River watersheds; together, this forms the largest estuary on the Pacific Coast. The whole estuary drains into the Pacific Ocean at the Golden Gate Bridge, while tides bring the saltwater of the Pacific Ocean into the bay creating a saline to freshwater gradient from the Golden Gate through San Pablo Bay, the Carquinez strait, Suisan Bay, and to the Delta (Figure 1). The Delta has been highly modified from a vast area of floodplains and marshes to leveed channels that export freshwater resources and protect islands from water incursion (Kimmerer, 2004; Moyle, 2002). The Bay-Delta provides habitat to 500 species of fish and wildlife, 20 of which are threatened or endangered (US EPA, n.d.).

Study species

Longfin Smelt is a small (<150 mm), pelagic, estuarine fish species that is distributed from California to Alaska (Merz et al., 2013; Moyle, 2002). A facultative anadromous species, across life stages they occupy the full gradient from freshwater to saltwater. In the San Francisco Bay-Delta, Longfin Smelt can be distributed throughout the estuary depending on the time of year and prevailing precipitation (Merz et al., 2013; Rosenfield & Baxter, 2007; Figure 1). During the winter and wetter parts of the year, spawning adults can be found moving in from the marine and brackish environments into low salinity and freshwater habitat from the South Bay to the Delta. Larvae have been found in fresh to brackish regions throughout the estuary in the winter/spring period (Grimaldo et al., 2020; Lewis et al., 2020). Juveniles tend to be distributed more seaward and become rarer in the upper estuary of the Delta and Suisun Bay during the summer period (Merz et al., 2013). In fall and winter, juveniles and spawning adults become more widely distributed throughout the estuary and most spawning takes place from February to April in tidal freshwater habitats (CDFW, 2018; Grimaldo et al., 2017; Merz et al., 2013; USFWS, 1996). Formerly abundant in the Bay-Delta, the Bay-Delta population is now listed as Endangered under the Endangered Species Act (ESA; 89 Fed. Reg. 61029; August 29, 2024). Declines have been attributed to myriad sources including decreased freshwater outflow, competition for zooplankton prey from invasive bivalves, loss of habitats for larval recruitment, increases in temperatures, and increased water clarity (Grimaldo et al., 2017; Hobbs et al., 2017; Kimmerer, 2008; Latour, 2016; Mac Nally et al., 2010; Moyle, 2002; Sommer et al., 2007; Thomson et al., 2010).

Data

To obtain fish count data, we used the R packages deltafish and LTMRdata that combine nine Bay-Delta fish monitoring program datasets (Bashevkin et al., 2022; Clark & Bashevkin, 2022). Among the datasets, three were suited to creating spatial dynamic multistate occupancy models for Longfin Smelt: Delta Smelt 20 mm (20 mm), Summer Tow Net (STN), and Fall Midwater Trawl (FMWT). These surveys together provide continuity for most of the year with the 20-mm covering spring (March–May; 8–10 survey periods), the STN covering summer (June–August; six survey periods), and the FMWT covering fall (September–December; four survey periods). While these monitoring programs sample a varying number of locations, a set of 30 sites are consistent between the three surveys and across years. For all three, the tow method is the same, but the net and mesh size are much larger for the FMWT than for the STN and 20 mm (Mitchell et al., 2019). For all three, a

21508925, 2025, 7, Downloaded from https://esajournals.onlinelibrary.wiley.com/doi/10.1002/ecs2.70326, Wiley Online Library on [14/07/2025]. See the Terms and Conditions (https://onlinelibrary.wiley.com/terms-and-conditions) on Wiley Online Library for rules of use; OA articles are governed by the applicable Creative Commons License

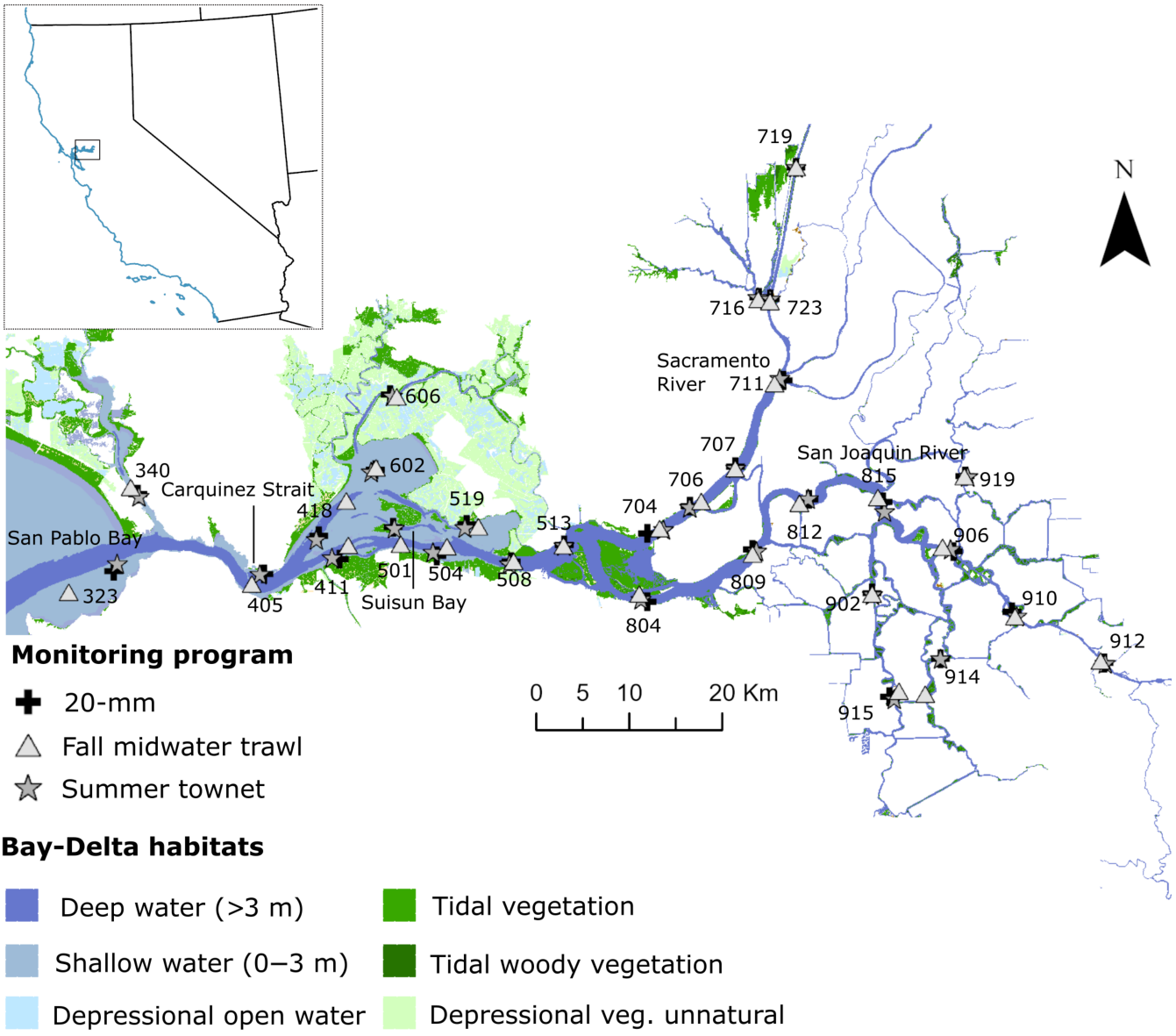

FIGURE 1 Locations of sites surveyed by the three monitoring programs in the San Francisco Bay-Delta used in this study. Thirty sites were consistent between the three monitoring programs. Site numbers are shown; in some cases, actual locations varied slightly as indicated by locations of symbols on the map.

stepped-oblique tow method is used, but the net and mesh size are much larger for the FMWT than for the STN and 20 mm (Mitchell et al., 2019). With stepped-oblique towing, the net is lowered to the bottom of the water being sampled and retrieved over a set time interval (usually 10–12 min); it is brought back to the surface in a stepped fashion where the rapid raising of the net is paused for consistent intervals of time. The maximum mouth area is 13.4 m^2 and the maximum mouth height is 3.7 m for the FMWT; the mesh size is 20.3 cm near the net mouth and 1.3 cm at the cod end. The maximum mouth area is 1.51 m^2 and the maximum mouth height is 1.2 m for the STN; the mesh size is 1.3 cm near the mouth and 2500 μm at the cod end. The maximum mouth area is 1.51 m^2 and maximum mouth height is 1.18 m for the 20-mm survey. The mesh size is 1600 μm. The 20-mm survey conducts three replicate tows for each visit to a site; the STN conducts two to three replicate tows for each visit (in the data we used, 59% of visits contained three replicates, the remainder contained two); the FMWT conducts one tow per visit.

We selected data from the most recent 11 years (2011–2021) to describe more recent Longfin Smelt population dynamics. We focused on this recent decade due to an earlier ecosystem shift cited by a stakeholder group (Peterson et al., 2024). We retained all available seasonal

21508925, 2025, 7, Downloaded from https://esajournals.onlinelibrary.wiley.com/doi/10.1002/ecs2.70326, Wiley Online Library on [14/07/2025]. See the Terms and Conditions (https://onlinelibrary.wiley.com/terms-and-conditions) on Wiley Online Library for rules of use; OA articles are governed by the applicable Creative Commons License

surveys from the STN and FMWT. For the 20-mm dataset, to mitigate interannual variation in capture probability due to interannual variation in larval sizes and size selectivity of the net, we filtered by length. As is done to filter the 20-mm dataset for the target species, Delta Smelt (*Hypomesus transpacificus*), we selected the five surveys each year that represented the first survey where Longfin Smelt measured 20 mm and the two prior and the two subsequent surveys. Survey 2 was not conducted in 2020 due to COVID-19 concerns, so we instead used survey 1. For 2014, where the size criterion was met by survey 1 (thus there were not two surveys prior), we used surveys 1–5. We created two datasets, leaving FMWT out of one dataset given that we had some uncertainty about the ability of the model to estimate detectability without replicate surveys, thus needing to condition on the underlying latent occupancy state. The "two-survey" dataset included data from 20 mm and STN. The "three-survey" dataset included data from 20 mm, STN, and FMWT.

To explain Longfin Smelt temporal distributions, we obtained environmental covariates related to surveys and stations (Table 1). We utilized environmental measurements collected during the surveys, including salinity, secchi depth, temperature, and water depth. Because tide data collected during the surveys were inconsistently collected, we downloaded tide height data from the National Ocean and Atmospheric Administration (NOAA) from the station at Port Chicago, CA (accessed September 9, 2022, at https://tidesandcurrents.noaa.gov/stationhome.html?id=9415144). Based on changes in tide height, we classified tides as slack, flood, and ebb. We used a height change of ≤0.016 m from a baseline height of 1.7 m in 6 min to indicate a slack tide, with flood tides or ebb tides exceeding that rate of change. We obtained estimates related to delta outflow from Dayflow, a hydrological model (accessed October 3, 2022, at https://data.cnra.ca.gov/dataset/dayflow). Dayflow estimates a suite of hydrological variables, including river inflows, river exports, as well as net delta outflow and X2. We considered both delta outflow and X2 but only consider delta outflow in models presented here, given the high correlation between the two and the greater improvement in deviance information criterion (DIC) in preliminary models when including delta outflow versus X2. Aquatic habitats have been found to correlate with stomach fullness for Delta Smelt, with a twofold increase in stomach fullness from the minimum (0 km^2) to the maximum (4.89 km^2) tidal wetland area (Hammock et al., 2019), which presumably impacts survival and reproduction. While not typically included as covariates in models of Bay-Delta fish distribution where water quality characteristics are favored, ours was an effort to include all possible available environmental drivers of distributions. Thus, we obtained information on aquatic habitats from the Delta Aquatic Resource Inventory (DARI) and Bay Area Aquatic Resource Inventory (BAARI) GIS layers (SFEI ASC [San Francisco Estuary Institute and Aquatic Science Center], 2017; SFEI, 2022). Based on exploratory analyses, we considered the following aquatic habitats: tidal vegetation, tidal woody vegetation, depressional unnatural vegetation (summed with the highly correlated depressional open water), tidal panne, woody slope unnatural, tidal channel, and tidal bay flat (Figure 1; Table 1). We calculated the proportion of cover of these habitat types in a buffer of 2 km surrounding each site based on the scale used to model Delta Smelt relationships to aquatic habitats (Hammock et al., 2019). To account for important variation related to survey when the survey was conducted, type, and effort, we also included covariates for survey source, number of days since the last survey, water year (the year beginning October 1, the start of the rainy season), day of year, and tow volume (Table 1).

Spatial dynamic multistate occupancy model

To estimate Longfin Smelt population dynamics, we used spatial dynamic multistate occupancy models describing three states: unoccupied (1), occupied by a relatively low number of individuals (hereafter *occupied*, 2), and occupied by a relatively high number of individuals (hereafter *abundant*, 3). We defined abundant using the 0.8 quantile of the distribution of counts, an optimized threshold from a simulation-based study (Steen et al., 2023). To find the threshold value, we combined the maximum counts obtained from each set of replicate tows from the three datasets into one dataset and determined the 0.8 quantile. If the count for a given replicate tow was greater than or equal to the threshold, we categorized it as abundant. We follow the notation used by Kéry and Royle (2020) and predecessors in describing the model parameters and indices. Thus, $y_{i,j,t}$ denotes the observed state at site i ($i = 1 \ldots M$), survey j ($j = 1 \ldots J$), and survey period t ($t = 1 \ldots T$), and $z_{i,t}$ represents the true latent occupancy state for site i at survey period t. The model only assumes that the true latent *occupancy* state does not change for a given survey period at a site; thus, it is robust to changes in the *numbers* of individuals present. The observation $y_{i,j,t}$ depends on the true occupancy state $z_{i,t}$ and detection probability $p_{i,j,t}$.

$$y_{i,j,t} \sim \mathrm{Cat}\left(z_{i,t} p_{i,j,t}\right).$$

21508925, 2025, 7, Downloaded from https://esajournals.onlinelibrary.wiley.com/doi/10.1002/ecs2.70326, Wiley Online Library on [14/07/2025]. See the Terms and Conditions (https://onlinelibrary.wiley.com/terms-and-conditions) on Wiley Online Library for rules of use; OA articles are governed by the applicable Creative Commons License

TABLE 1 Summary statistics for explanatory covariates included in global Longfin Smelt multistate occupancy models.

Description	Summary
Detection probability models: p	
Survey source: 20 mm, STN, or FMWT	20 mm = 4783; STN = 5117; FMWT = 1199
Volume of water sampled by the tow (m^3)	20 mm: $\overline{X}$ = 921 (134; 222, 1426) STN: $\overline{X}$ = 682 (61; 26, 1479) FMWT: $\overline{X}$ = 5046 (890; 2711, 8560)
State transition probability models: ϕ, ρ	
No. days since the last survey at that location	Two survey: $\overline{X}$ = 32 (58.5; 4, 246) Three survey: $\overline{X}$ = 24 (24.7; 4, 142)
Day of the year	Two survey: $\overline{X}$ = 160 (44.8; 75, 241) Three survey: $\overline{X}$ = 175 (61.2; 75, 352)
Bottom depth: recorded at time of tow or an average for that location (m)	Two survey: $\overline{X}$ = 8.1 (3.6; 0.3, 21.6) Three survey: $\overline{X}$ = 8.3 (3.7; 0.3, 22.9)
Salinity measured at the water surface ($\mu s/cm^3$)	Two survey: $\overline{X}$ = 3.2 (5.5; 0.0, 27.3) Three survey: $\overline{X}$ = 3.4 (5.6; 0.0, 27.8)
Water temperature measured at the water surface (°C)	Two survey: $\overline{X}$ = 20 (3.0; 12, 29) Three survey: $\overline{X}$ =19 (3.2; 7, 29)
Estimate of daily delta outflow (cfs)	Two survey: $\overline{X}$ = 19,010 (26,119; 2263, 131,167) Three survey: $\overline{X}$ = 17,884 (25,051; 1981, 131,167)
Tide direction: Flood (I), ebb (D), or slack (S)	Two survey: I = 2842, S = 4405, D = 2653 Three survey: I = 3230, S = 4982, D = 2887
Tidal vegetation: Proportion of natural vegetated tidal habitat in a 2-km radius surrounding survey station (tv)	Two survey: $\overline{X}$ = 0.06 (0.08; 0.00, 0.30) Three survey: $\overline{X}$ = 0.06 (0.08; 0.00, 0.30)
Depressional vegetated and non-vegetated unnatural: Small artificially impounded water bodies with no tidal connection and the vegetated areas adjacent to open water (dvwu)	Two survey: $\overline{X}$ = 0.05 (0.15; 0.00, 0.79) Three survey: $\overline{X}$ = 0.05 (0.15; 0.00, 0.79)
Woody slope unnatural: Slope wetland with woody vegetation in modified environments; commonly along levees (fsu)	Two survey: $\overline{X}$ = 0.004 (0.009; 0.000, 0.041) Three survey: $\overline{X}$ = 0.004 (0.009; 0.000, 0.041)
Tidal Marsh Panne Natural: Unvegetated ponds in marsh plain (tp)	Two survey: $\overline{X}$ = 0.001 (0.005; 0.000, 0.026) Three survey: $\overline{X}$ = 0.001 (0.004; 0.000, 0.026)
Tidal channel natural (tc)	Two survey: $\overline{X}$ = 0.015 (0.15; 0.00, 0.57) Three survey: $\overline{X}$ = 0.15 (0.15; 0.00, 0.57)
Tidally connected willow wetland (tvw)	Two survey: $\overline{X}$ = 0.006 (0.013; 0.00, 0.074) Three survey: $\overline{X}$ = 0.007 (0.013; 0.000, 0.074)
Bay flat: Occurs between mean tide level and mean lower low water, not channelized with little vegetation (tbf)	Two survey: $\overline{X}$ = 0.007 (0.012; 0.00, 0.045) Three survey: $\overline{X}$ = 0.006 (0.012; 0.000, 0.045)
Detection and transition probability models	
Secchi depth (cm)	Two survey: $\overline{X}$ = 75 (47.5; 7, 300) Three survey: $\overline{X}$ = 78 (51.1; 7, 470)

Note: For continuous variables, parentheses contain the SD followed by the minimum and maximum values. Two survey refers to the dataset containing the combined 20 mm and STN surveys; and three survey refers to the dataset containing 20 mm, STN, and FMWT surveys.
Abbreviations: FMWT, Fall Midwater Trawl; STN, Summer Tow Net.

Detection probability depends on whether the true state is two or three. We assumed no false positives where a higher state is detected than the true state (e.g., state 3 is never detected when the true state is two) and modeled conditional detection probability as p_2 (the probability of detecting state 2 given true state 2), p_{32} (the probability of detecting state 2 given true state 3), and p_{33} (the probability of detecting state 3 given true state 3). We modeled these three parameters with logit-linear models as follows:

$$\text{logit}\left(p_{2_{i,j,t}}\right) = \beta_0 + \beta_1 \text{STN}_{i,t} + \beta_2 \text{FMWT}_{i,t} + \beta_3 \text{secchi}_{i,t} + \beta_4 \text{tow volume}_{i,j,t},$$

21508925, 2025, 7, Downloaded from https://esajournals.onlinelibrary.wiley.com/doi/10.1002/ecs2.70326, Wiley Online Library on [14/07/2025]. See the Terms and Conditions (https://onlinelibrary.wiley.com/terms-and-conditions) on Wiley Online Library for rules of use; OA articles are governed by the applicable Creative Commons License

where β is the parameter estimates, STN and FMWT are the binary indicator variable for samples collected with the STN and FMWT, respectively, and secchi and tow volume are described above. The global model is shown only for p_2; the same global model was used for p_{32} and p_{33}.

Conditional on the true occupancy state (rows), the probability of detecting the three states (columns) was according to the following matrix Θ (theta):

$$\Theta_{z,o} = \begin{bmatrix} 1 & 0 & 0 \\ 1-p_2 & p_2 & 0 \\ 1-p_{32}-p_{33} & p_{32} & p_{33} \end{bmatrix}$$

We estimated initial site-level (i) multistate occupancy by modeling the probability of being occupied (ψ, occupancy probability regardless of abundance state) and abundant (r, the probability of an occupied site being in the abundant state) as a logit-linear function of estimated spatial relationships:

$$\text{logit}\left(\psi_{i,t=1}\right) = \alpha + \text{smooth}_i.$$

The same model structure was used for r, where α is the intercept and smooth is a spatial smooth. We used thin-plate splines to estimate two-dimensional (spatial) smooths (Collier et al., 2012). We used 20 knots from which to estimate spatial relationships. As suggested by Kéry and Royle (2020), we mean centered the estimated smooth, so it is not confounded with the intercept of the model.

The latent initial site-level occupancy states were categorically distributed, given the probabilities of not being occupied $(1-\psi_{i,t=1})$, being occupied $(\psi_{i,t=1}(1-r_{i,t=1}))$, and being abundant $(\psi_{i,t=1}r_{i,t=1})$, states 1, 2, and 3, respectively, as follows:

$$z_{i,t=1} \sim \text{Cat}\left(1-\psi_{i,t=1}, \psi_{i,t=1}(1-r_{i,t=1}), \psi_{i,t=1}r_{i,t=1}\right).$$

Given initial occupancy, subsequent occupancy estimates were modeled using six transition probability parameters to describe transition probabilities between the three states: ϕ_x is the probability that a site (i) is occupied at survey period t given state x in the previous survey period $(t-1)$, and ρ_x is the conditional probability that an occupied site is abundant given state x in the previous survey period. We described global models to explore the effects of aquatic habitats, water quality characteristics, tide, and day of year while accounting for residual spatial and temporal autocorrelation (see Table 1 for variables and definitions). We modeled the water quality characteristics with randomly varying slopes at the site level because we expected relationships to vary depending on location given the varying range of these covariates by site. For example, salinity ranges at a brackish site cover larger values than salinity ranges at a freshwater site; thus, the juvenile or sub-adult life stage which may prefer moderate salinity might respond negatively to salinity changes at brackish sites and positively at freshwater sites. With respect to outflow—which does not vary by site—bigger outflow events may move fish outward in the estuary which may result in increases at some sites and decreases at others. We included a spatial smooth for each parameter as described for initial occupancy to account for spatial autocorrelation and a random effect of water year on the six transition probabilities to account for unexplained temporal variation. The state transition parameters: ϕ_1 (probability of becoming occupied given unoccupied at time $t-1$), ϕ_2 (probability of staying occupied given occupied at time $t-1$), ϕ_3 (probability of being occupied given occupied in the abundant state at time $t-1$), ρ_1 (conditional probability of becoming abundant given unoccupied at time $t-1$), ρ_2 (conditional probability of becoming abundant given occupied at time $t-1$), and ρ_3 (conditional probability of staying abundant given abundant at time $t-1$) were modeled as a logit-linear function of the model parameters (only ϕ_1 is shown here):

$$\text{logit}\left(\phi_{1i,t}\right) = \beta_{0,j} + \beta_{1,i}x_{1,i,t} + \ldots + \beta_{Q,i}x_{Q,i,t} + \text{smooth}_i.$$

The randomly varying intercept was assumed normally distributed with mean γ and variance τ.

Site-level occupancy states (columns) for time periods $t > 1$ were governed by transition probabilities given occupancy during the previous time step (rows) according to the following matrix Φ:

$$\Phi_{z(t-1),z(t)} = \begin{bmatrix} 1-\phi_1 & \phi_1(1-\rho_1) & \phi_1\rho_1 \\ 1-\phi_2 & \phi_2(1-\rho_2) & \phi_2\rho_2 \\ 1-\phi_3 & \phi_3(1-\rho_3) & \phi_3\rho_3 \end{bmatrix}$$

Estimated occupancy for site i at time t for $t > 1$ is then categorically distributed as follows:

$$z_{i,t} \mid z_{i,t-1} \sim \text{Cat}\left(\Phi_{z(t-1),z(t),i,t}\right).$$

Because we considered covariate rich global models, we used a variable selection procedure to aid inference. We used Gibbs variable selection, where the priors for the coefficients θ_j depend on Bernoulli distributed indicator variables ω_j as follows:

$$\theta_j \mid \omega_j \sim \omega_j\text{Norm}\left(0, \tau^2\right) + \left(1-\omega_j\right)\text{Norm}\left(\mu_{\text{tune}}, \sigma_{\text{tune}}\right).$$

We chose the tuning parameters $(\mu_{\text{tune}}, \sigma_{\text{tune}})$ to be near the posteriors for each coefficient (Dellaportas

21508925, 2025, 7, Downloaded from https://esajournals.onlinelibrary.wiley.com/doi/10.1002/ecs2.70326, Wiley Online Library on [14/07/2025]. See the Terms and Conditions (https://onlinelibrary.wiley.com/terms-and-conditions) on Wiley Online Library for rules of use; OA articles are governed by the applicable Creative Commons License

et al., 2002). Thus, we fit the global model to obtain the tuning parameters for each coefficient before fitting models using Gibbs variable selection. Using tuned priors does not influence the posterior for θ_j as might be expected, but it rather improves the behavior of the MCMC algorithm (Hooten & Hobbs, 2015). We first ran the group of detection models (p_2, p_{32}, p_{33}) and then ran the transition probability models one submodel at a time in the following order: ρ_3, ρ_2, ρ_1, ϕ_3, ϕ_2, ϕ_1. At each step, we first fit the global submodel to obtain posteriors for the tuning parameters and then ran the model with variable selection. Once the important variables were identified—as those with indicator posterior estimates greater than the prior—we retained those variables and proceeded to the next submodel. In the procedure, other submodels were estimated using an intercept only, unless variables had been selected for that submodel, in which case the submodel was specified using the selected variables. Once all important variables were identified for all submodels, we reran the full model with uninformative priors and we present intercept and coefficient estimates based on that final model.

We ran our analyses in R (R Core Team, 2023) using JAGS (version 4.3.0, Plummer, 2003) via the R package jagsUI (version 1.5.2, Kellner, 2018). To compute the spatial coverage design for the spatial smooth, we use the R package fields (Nychka et al., 2021). We used the jagsUI function autojags to run submodels to convergence ($\widehat{R} \leq 1.1$). We specified 1000 burn-in, 3 chains, and otherwise used the default autojags settings. The final three-survey model ran for 168,000 iterations, while the final two-survey model ran for 162,000 iterations. We standardized all continuous covariates to have a mean of 0 and SD of 1. For any missing values for salinity, temperature, secchi, and delta outflow, we substituted the average standardized values for the prior and subsequent surveys for that station. We standardized tow volume by survey source (i.e., within group standardization following, Raudenbush & Bryk, 2002); for any missing values, we substituted the average standardized values across stations for that survey period. The aquatic habitat covariates, which only varied spatially, did not have any missing values.

To aid interpretation, in addition to coefficient estimates, we report odds ratios for covariates in the final transition probability models (Mackenzie et al., 2006). Because continuous covariates were standardized, odds ratios reflect one SD change in continuous covariates. For year random effects, we report median odds ratios following Larsen et al. (2000). To calculate median odds ratios for spatial random effects, we followed a similar approach and calculated odds ratios between all pairs of stations, dividing the larger value by the smaller value. We then calculated the median value of these odds ratios.

RESULTS

The three-survey dataset had 4776 total primary occasions conducted across 11 years, with 15 surveys per year (except in 2021 where there were 11) conducted at 30 sites minus missed surveys (Appendix S1: Table S1). The 0.8 quantile of non-zero counts was 21, and thus, replicate tows were classified as abundant if at least 21 individuals were captured. Naïve occupancy estimates indicated that sites were occupied in 15.5% ($n = 741$) of the primary occasions with 3.2% ($n = 152$) occupied in the abundant state (Figure 2). Occupancy models, which estimated occupancy for sites while accounting for imperfect detection, and even if the survey was not conducted, estimated occupancy for a total of 4832 primary occasions. Sites were estimated to be occupied for 25.2% ($n = 1219$) of surveys, with 5.7% ($n = 274$) occupied in the abundant state (Figure 2).

Occupancy

The two-survey and three-survey datasets produced similar results; thus, we present results for the three-survey dataset in the main body of the paper and results for the two-survey dataset in Appendix S1. Initial mean (across sites) probability of occupancy was 0.29 (CI: 0.08, 0.55), and initial mean probability of being in the abundant state was 0.13 (CI: 0.01, 0.44). There was variation in the parameters that influenced each of the six transition probabilities (Table 2). The day of year was important for five of the six transition probability parameters. There also was strong evidence that the changes in occupancy through time were quadratic rather than linear. There was little-to-no evidence that the state transition probabilities were related to environmental variables salinity, surface water temperature, delta outflow, and secchi depth as evidenced by the small posterior indicator variable means (Table 2). By contrast, ebb tide was selected for two transition models, but the evidence for flood tide was weaker. Bottom depth was positively related to the conditional probability of staying abundant (ρ_3) or becoming abundant once occupied (ρ_2). A number of habitat covariates were important to remaining (ρ_3) or becoming abundant (ρ_2); this included unnatural woody slopes (negative relationship), willow wetlands (negative relationship), and tidal bay flats (positive relationship) (Table 2). While the variable selection procedure did not always select the number of days since the last survey,

21508925, 2025, 7, Downloaded from https://esajournals.onlinelibrary.wiley.com/doi/10.1002/ecs2.70326, Wiley Online Library on [14/07/2025]. See the Terms and Conditions (https://onlinelibrary.wiley.com/terms-and-conditions) on Wiley Online Library for rules of use; OA articles are governed by the applicable Creative Commons License

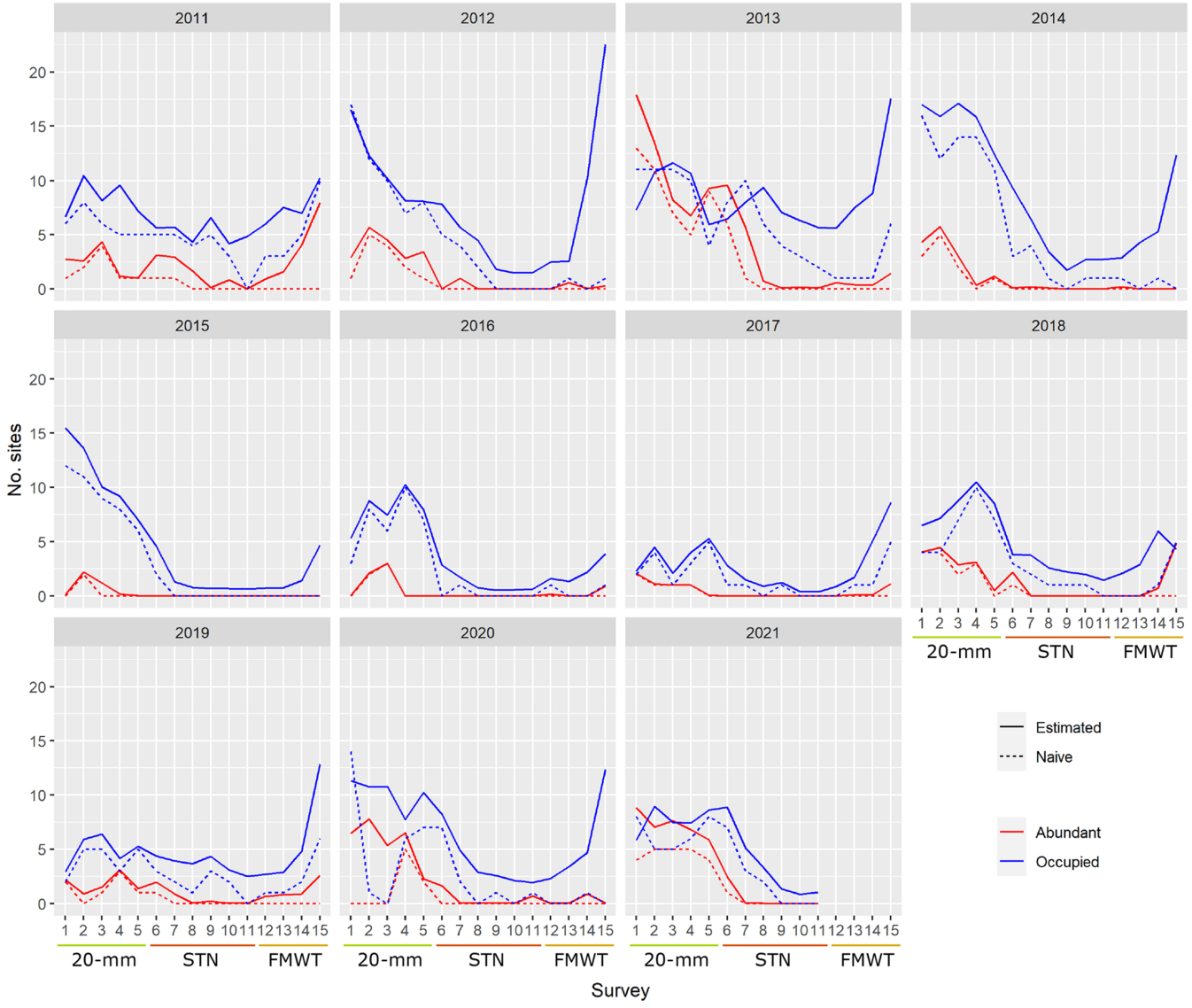

FIGURE 2 Naïve and estimated multistate occupancy for the three-survey dataset (20-mm survey, Summer Tow Net [STN], and Fall Midwater Trawl [FMWT]) showing the number of sites (out of 30) that were occupied or abundant across 15 survey periods per year.

we retained this covariate in all final transition probability models because it addressed sampling variation of known importance (i.e., the variation in the number of days since the last survey).

The probabilities of becoming occupied if previously unoccupied or occupied (ϕ_1, ϕ_2) were highly dependent on the day of year as well as the random effects of year and space as evidenced by the large median odds ratios (Table 3, Figures 3 and 4). Spatial estimates indicated that these probabilities increased for sites near or past the confluence of the rivers (Figures 3 and 5); however, the overall picture varied by season with sites upriver estimated to be occupied depending on season and year (Figure 5; Appendix S1: Figures S15–25). The probability of becoming abundant if occupied or staying abundant (ρ_2, ρ_3) was most strongly influenced by woody habitats (3- to 10-fold lower likely with a 1 SD increase; Table 4, Figure 4) with relatively smaller effects of depth, day of year, and the random effects of year and space (Figures 3 and 4).

Detection

The estimated probability of detecting occupancy, given that a site was occupied in the non-abundant state (p_2), for the 20-mm survey was 0.21 (CI: 0.15, 0.29; Table 5). The estimated probability of detecting occupancy given the abundant state (p_{32}) in the 20-mm survey was 0.66 (CI: 0.57, 0.75), and the probability of detecting abundant given the abundant state (p_{33}) was 0.31 (CI: 0.23, 0.41). Detection probabilities p32 and p33 were derived using a multinomial logit link based on posterior samples of the

21508925, 2025, 7, Downloaded from https://esajournals.onlinelibrary.wiley.com/doi/10.1002/ecs2.70326, Wiley Online Library on [14/07/2025]. See the Terms and Conditions (https://onlinelibrary.wiley.com/terms-and-conditions) on Wiley Online Library for rules of use; OA articles are governed by the applicable Creative Commons License

TABLE 2 Posterior means of indicator variables for the explanatory variables in global models for the spatial dynamic multistate occupancy models.

	Transition parameters						Detection parameters		
Variable	ϕ_1	ϕ_2	ϕ_3	ρ_1	ρ_2	ρ_3	p_2	p_{32}	p_{33}
Source							**1.00, 1.00**	**1.00, 1.00**	**1.00, 1.00**
Tow volume							0.03	**0.53**	**0.52**
No. days since last survey	0.25	**0.54**	0.49	**0.92**	0.41	**0.72**			
Day of the year	**0.53**	0.44	**0.86**	0.44	**0.84**	0.33			
Day of the year^2	**0.94**	**1.00**	**1.00**	0.25	**0.98**	**0.99**			
Bottom depth	0.06	0.14	0.31	0.27	**0.52**	**0.90**			
Salinity	0.00	0.00	0.00	0.14	0.00	0.00			
Secchi depth	0.00	0.00	0.00	0.14	0.15	0.00	**1.00**	**1.00**	**1.00**
Surface water temperature	0.00	0.00	0.00	0.17	0.00	0.02			
Delta outflow	0.00	0.00	0.00	0.12	0.09	0.00			
Flood tide	0.08	0.13	0.45	0.46	0.13	0.15			
Ebb tide	0.47	**0.98**	**0.58**	0.49	0.43	0.27			
Tidal vegetation	0.07	0.11	0.34	0.26	0.06	0.17			
Depressional vegetated and non-vegetated unnatural	0.03	0.16	0.24	0.23	0.06	0.05			
Woody slope unnatural	0.08	0.12	0.47	0.23	0.12	**0.97**			
Tidal marsh panne natural	0.03	0.06	0.49	0.34	0.10	0.06			
Tidal channel	0.05	0.08	0.36	0.31	0.31	0.10			
Tidally connected willow wetland	0.13	0.22	0.49	0.30	**0.54**	**0.85**			
Bay flat	0.05	0.15	0.49	0.33	**0.72**	0.08			

Note: The three-survey dataset results are presented here (see Appendix S1: Table S2 for the two-survey dataset results). Means >0.5 (the prior probability for the indicator) are indicative of an important variable and are shown in boldface.

intercepts (i.e., baseline detection, assuming centered covariates). Secchi depth had a big effect on detection; for example, with one SD increase in secchi depth (+51 cm), the probability of detecting occupancy in the non-abundant state decreased from 0.21 to 0.03 (CI: 0.02, 0.05) for the 20-mm survey. In the STN survey, detection probabilities decreased for p_2 to 0.06 (CI: 0.03, 0.09), increased for p_{32} to 0.72 (CI: 0.51, 0.89), and decreased for p_{33} to 0.05 (CI: 0.02, 0.09). The probability of detecting occupancy, given that a site was occupied in the non-abundant state, was lower for the FMWT survey than for the 20-mm survey ($p_2 = 0.05$; CI: 0.02, 0.10); given the abundant state, the probability of detecting occupancy was very high ($p_{32} = 0.97$; CI: 0.74, 1.00), but the probability of detecting the abundant state was very low ($p_{33} = 0.005$; CI: 0.00, 0.03).

For the three detection probability parameters, the survey source was always selected, as was secchi depth (Table 5). While tow volume was not always selected, we retained this covariate in all models given the inherent relationship between variation in fish counts and variation in the volume of water sampled.

DISCUSSION

Imperiled fish and wildlife species need statistically sound insights to guide efficacious management actions. We demonstrated the use of a spatial dynamic multistate occupancy approach for a once common, but now rare, fish, the Bay-Delta population of the Longfin Smelt. Our approach achieved and validated a number of objectives relevant to many systems including disentangling the impact of variables on detectability versus their impact on occupancy, understanding the drivers of high versus low abundance, understanding the dynamics of the population, and gaining insight into information gaps where environmental variables may be missing. Compared to the normal metric utilized for insights into Longfin Smelt populations—a static annual population index—our approach allowed us to elucidate a complex picture of a highly dynamic fish population with unspecified broad-scale forces (random effects of year and space) relating to occupancy and local habitat features relating to abundance.

21508925, 2025, 7, Downloaded from https://esajournals.onlinelibrary.wiley.com/doi/10.1002/ecs2.70326, Wiley Online Library on [14/07/2025]. See the Terms and Conditions (https://onlinelibrary.wiley.com/terms-and-conditions) on Wiley Online Library for rules of use; OA articles are governed by the applicable Creative Commons License

TABLE 3 Mean estimates, SD, upper and lower 95% credible intervals, and odds ratios (ORs) or median ORs for random effects for occupancy state transition probabilities for the three-survey dataset (see Appendix S1: Table S3 for the two-survey dataset).

Parameter	Mean	SD	Lower 95%	Upper 95%	OR
Probability of becoming occupied if unoccupied, ϕ_1					
Intercept	−3.66	0.48	−4.64	−2.78	
Year random effect (SD)	0.95	0.31	0.52	1.69	2.53
Spatial smooth (min. estimate) (site 912)	−2.44	0.78	−4.09	−1.02	
Spatial smooth (max. estimate) (site 501)	1.08	0.22	0.65	1.52	
Spatial random effect (OR only)					2.50
No. days since last survey	−1.00	0.62	−2.37	−0.04	0.37
Day of the year	0.17	0.21	−0.24	0.58	1.19
Day of the year^2	1.10	0.20	0.70	1.48	3.00
Probability of remaining occupied if occupied, ϕ_2					
Intercept	−2.22	0.64	−3.54	−1.04	
Year random effect (SD)	0.48	0.32	0.03	1.24	1.94
Smooth (min. estimate) (site 912)	−4.38	2.12	−8.96	−0.55	
Smooth (max. estimate) (site 405)	2.33	0.56	1.31	3.50	
Spatial random effect (OR only)					6.26
No. days since last survey	0.25	0.72	−1.07	1.76	1.28
Day of the year	0.01	0.44	−0.88	0.86	1.01
Day of the year^2	1.73	0.40	0.98	2.55	2.99
Ebb tide	0.78	0.33	0.15	1.46	2.19
Probability of remaining occupied if abundant, ϕ_3					
Intercept	1.67	1.84	−1.47	5.77	
Year random effect (SD)	4.54	2.28	0.95	9.42	7.62
Smooth (min. estimate) (site 912)	−1.18	3.60	−12.00	2.03	
Smooth (max. estimate) (site 340)	1.15	2.91	−1.03	9.62	
Spatial random effect (OR only)					1.87
No. days since last survey	−0.99	0.96	−2.90	0.86	0.37
Day of the year	−2.57	1.18	−4.94	0.32	0.08
Day of the year^2	1.59	1.20	−0.85	3.86	4.89
Ebb tide	0.64	1.16	−1.56	3.03	1.89

Note: Transitional probabilities are conditional on the occupancy state during the previous survey.

Modeling detectability allowed us to disentangle the effects of visibility (modeled as secchi depth) on detectability versus site occupancy. While imperfect detectability can be problematic for estimating true population size by producing undercounts of actual numbers, it can also bias estimated environmental relationships (Tyre et al., 2003). In the Bay-Delta, studies have found that sites with increased secchi depth have correlated with low fish abundance (Latour, 2016; Mahardja et al., 2017; Sommer & Mejia, 2013). However, it has also been acknowledged (Latour, 2016) or found (Peterson & Barajas, 2018) that sites with increased secchi depth have reduced *detectability* and not necessarily lower abundance or occupancy rates. In our analysis, this variable consistently related to reduced detectability across occupancy states, indicating that this variable should be included in any population calculations for Longfin Smelt or possibly similar fish in the Bay-Delta. The fact that this variable was not selected in occupancy models but was consistently retained in detectability models suggests that Longfin Smelt occupancy at sites with higher water clarity is not affected, but that detection is reduced—possibly due to behavioral responses to increased visibility in the water column. Other fish studies have found a similar effect, underscoring the importance of explicitly

21508925, 2025, 7, Downloaded from https://esajournals.onlinelibrary.wiley.com/doi/10.1002/ecs2.70326, Wiley Online Library on [14/07/2025]. See the Terms and Conditions (https://onlinelibrary.wiley.com/terms-and-conditions) on Wiley Online Library for rules of use; OA articles are governed by the applicable Creative Commons License

addressing detectability in aquatic systems (e.g., Guest et al., 2003; Kaartvedt et al., 2012; Rakowitz et al., 2012).

Knowledge of the environmental drivers of higher (or lower) abundance can lead to more effective management strategies than simply targeting areas of occurrence by ensuring that the most critical habitats are conserved or the most critical threats are mitigated (Howard et al., 2014; Pearce & Ferrier, 2001). Given variation in counts, we were able to differentiate sites with low abundance versus those with high abundance; we found different correlates of high abundance, thus gaining insights that may have been unavailable in a basic (two state) occupancy model. Because the high abundance state sites reflected a relatively small portion of the occupied sites, it is reasonable to think that by pooling those data with the low abundance sites in a basic occupancy model, the pattern in the low abundance sites would drive the results. The finding that habitat variables were frequently important to transitioning to or staying in the abundant state, but not the occupied state, could be that—once established through the broad-scale forces described by year, day, and spatial smooth—better habitats support larger populations of fish. In fact, the negative relationships we found with woody habitat (here, *tvw* and *fsu*) and the abundant state could indicate areas of higher depredation or avoidance of predators (Moyle, 2002; Moyle et al., 2011; USFWS, 1996). This finding is, as far as we are aware, novel for the system and of potential management relevance. Increasing bottom depth likely supports abundance as an artifact of referencing sites that retain water through tidal fluctuations.

Statistical modeling in ecology always involves reducing complex systems to the components that are known, quantifiable, and estimable (Hooten & Hobbs, 2015). With a dynamic occupancy model, we could estimate when occupancy of sites changed throughout the year,

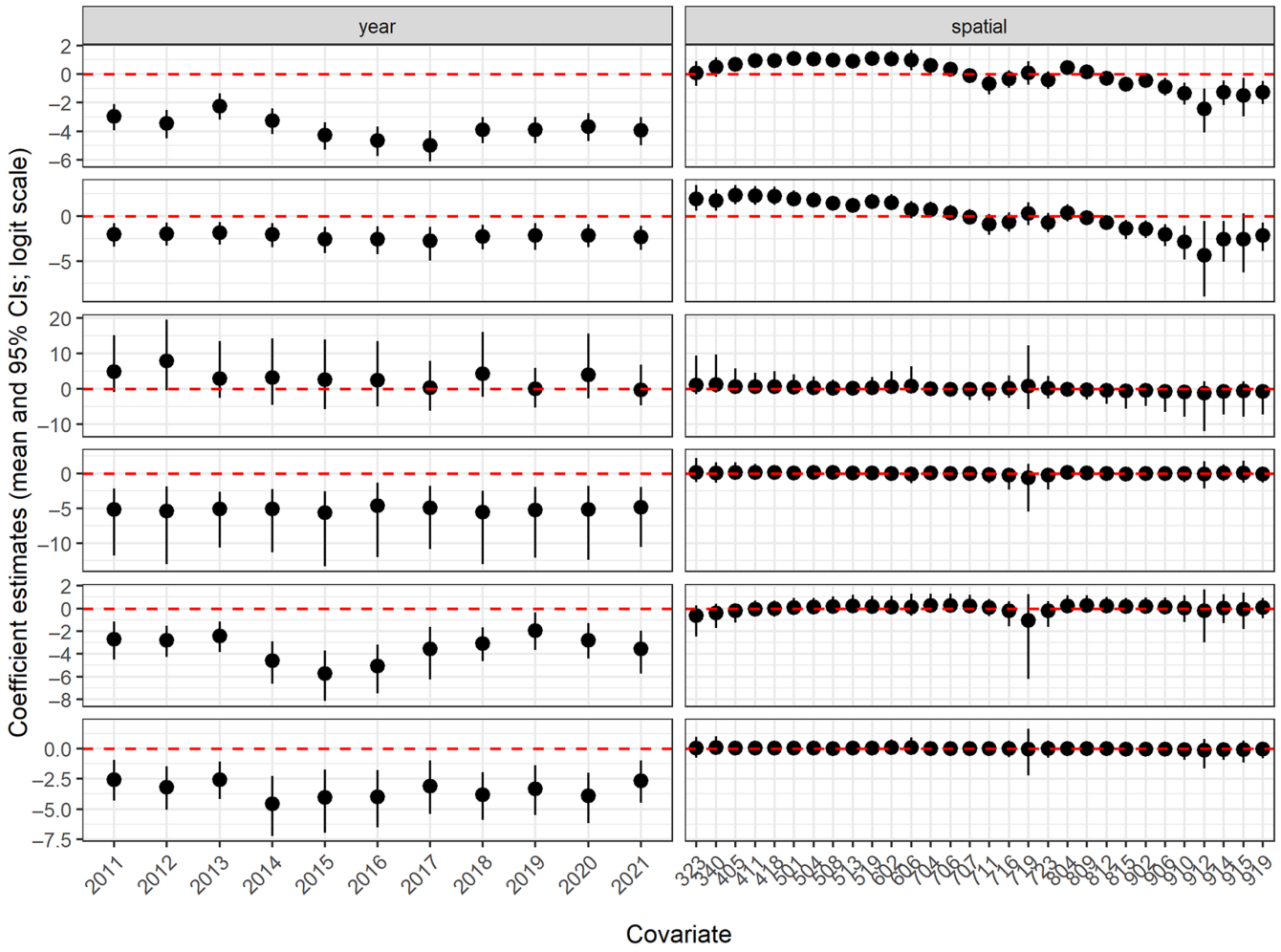

FIGURE 3 Coefficient estimates (solid circles) are shown with 95% credible intervals for each transition probability parameter for the random effect of water year, estimated site-level spatial effect given a spatial smooth, and the selected fixed effects (*n*days, the number of days since last survey, was included in all models) for the three-survey dataset. For spatial plots, sites are ordered generally from west to east on the *x*-axis (see Figure 1 for the exact location of each site). See Appendix S1: Figure S2 for the equivalent table for the two-survey dataset.

21508925, 2025, 7, Downloaded from https://esajournals.onlinelibrary.wiley.com/doi/10.1002/ecs2.70326, Wiley Online Library on [14/07/2025]. See the Terms and Conditions (https://onlinelibrary.wiley.com/terms-and-conditions) on Wiley Online Library for rules of use; OA articles are governed by the applicable Creative Commons License

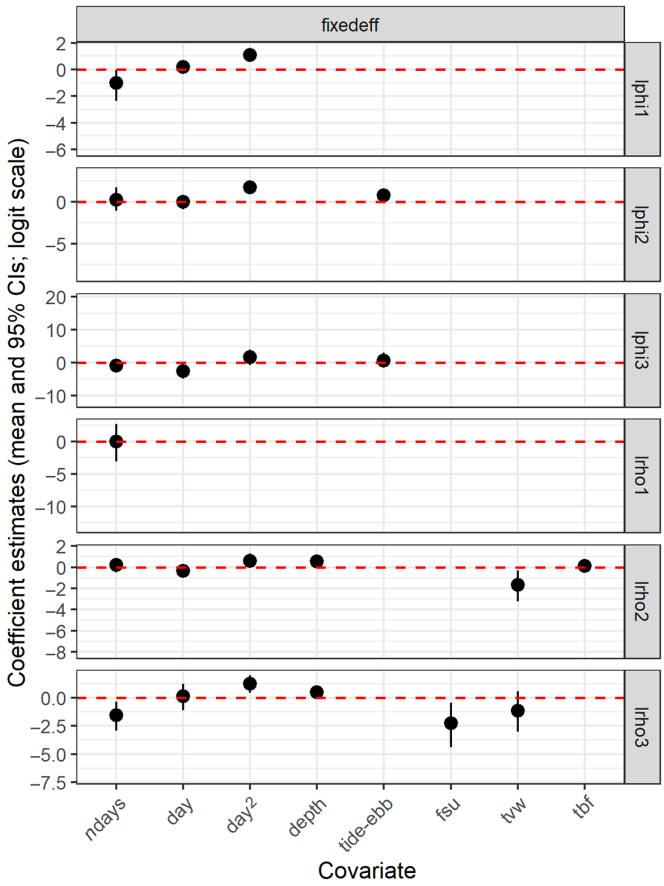

FIGURE 3 (Continued)

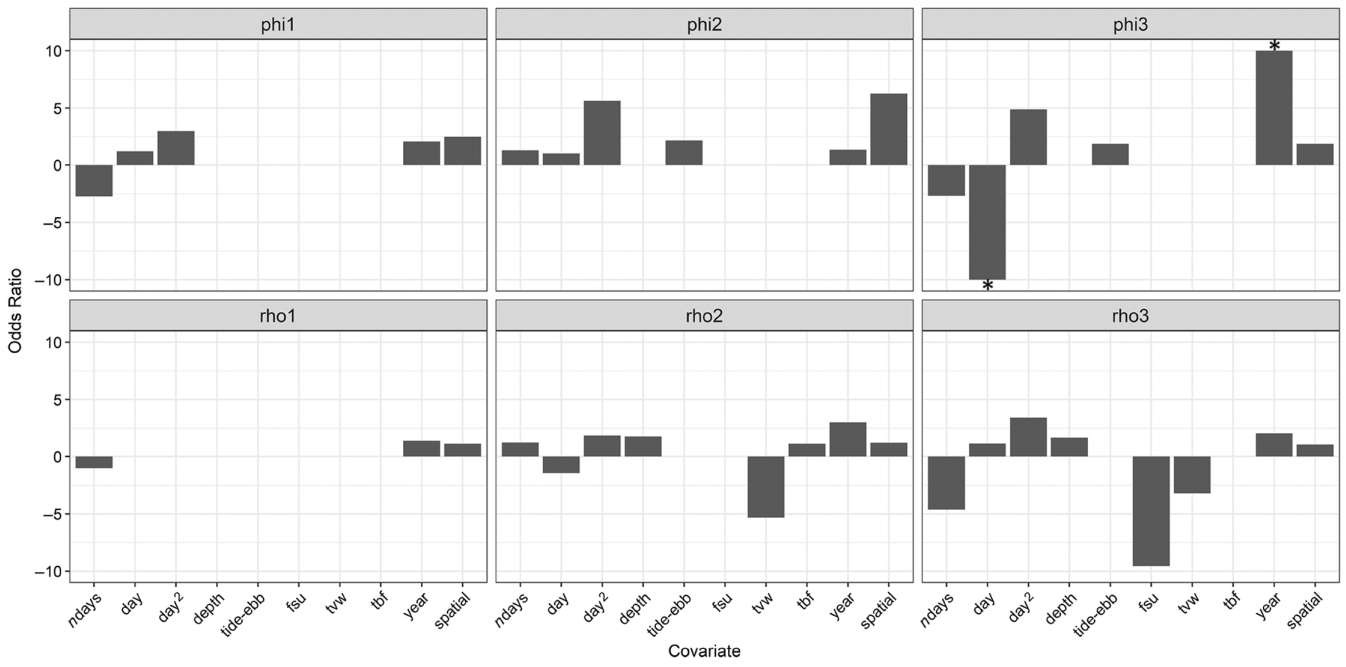

FIGURE 4 Odds ratios for covariates from Figure 3. Fixed-effect covariates were selected using indicator variables (Table 2). Median odds ratios are shown for the random year effect and the spatial smooth. The one value less than −10 was truncated at −10.

21508925, 2025, 7, Downloaded from https://esajournals.onlinelibrary.wiley.com/doi/10.1002/ecs2.70326, Wiley Online Library on [14/07/2025]. See the Terms and Conditions (https://onlinelibrary.wiley.com/terms-and-conditions) on Wiley Online Library for rules of use; OA articles are governed by the applicable Creative Commons License

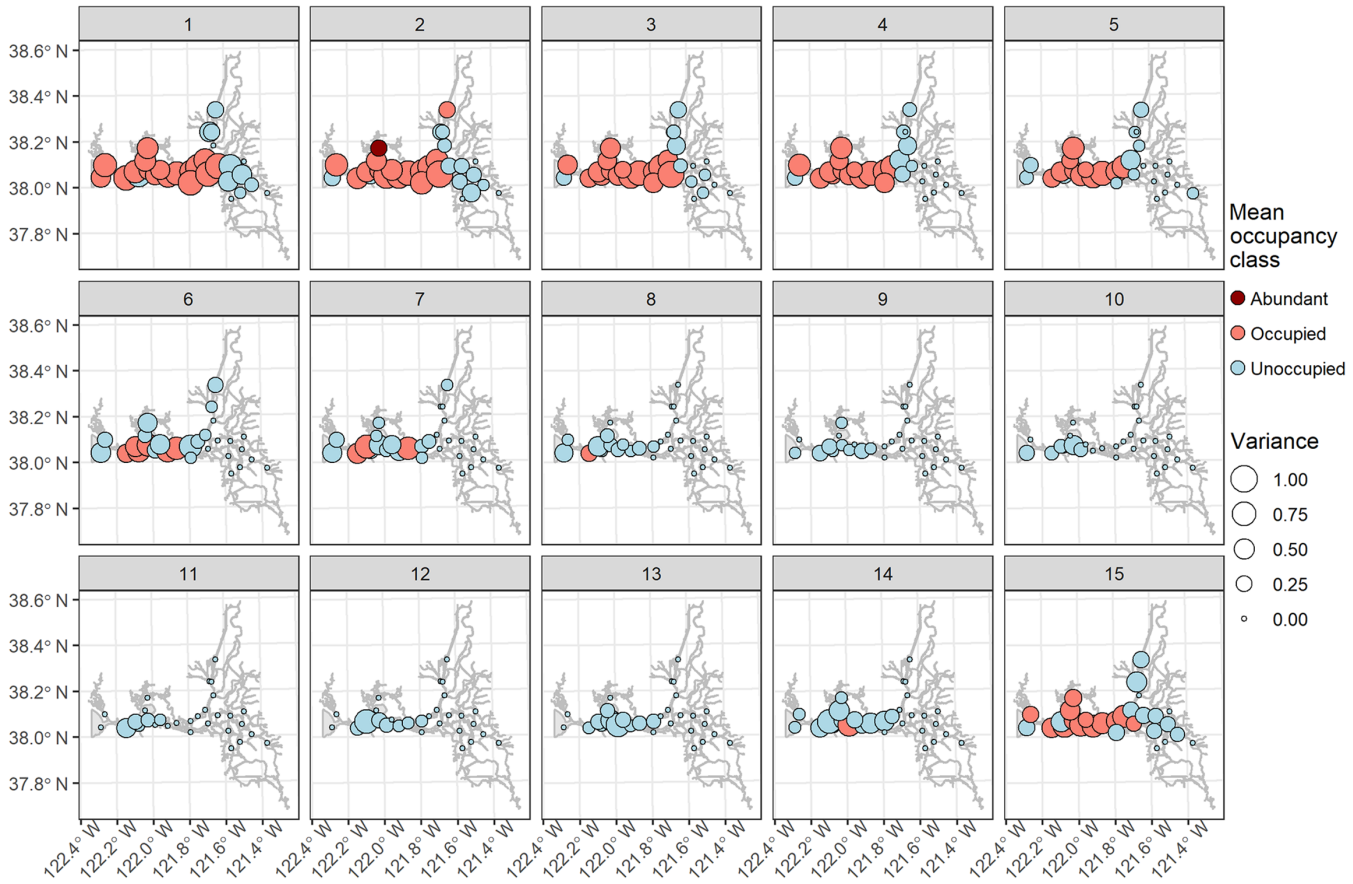

FIGURE 5 Mapped mean and variance in estimated occupancy classes across 11 years (2011–2021) for each of 15 survey periods and 30 survey stations. Survey periods 1–5 correspond to spring (20-mm survey), 6–11 to summer (Summer Tow Net [STN] survey), and 12–15 to fall (Fall Midwater Trawl [FMWT] survey). For maps showing yearly estimated and actual occupancy, see Appendix S1: Figures S4–S25.

explore why they changed, and allow inclusion of frequent surveys that were temporally autocorrelated (MacKenzie et al., 2009). Numerous previous studies have found that abiotic variables—environmental covariates describing temperature, salinity, secchi depth, as well as a hydrological covariate (we included an estimate of Delta outflow)—were important to Longfin Smelt distributions (Duarte & Peterson, 2021; Mahardja et al., 2017; Nobriga & Rosenfield, 2016; Peterson & Barajas, 2018). None of these covariates were selected in our variable selection procedure. The USFWS in a 1996 report stated that "the positive relationship between Longfin Smelt abundance and outflow may have broken down in recent years, or dropped to a lower level" (USFWS, 1996), indicating that at least one previously important abiotic relationship has not withstood changes in the Bay-Delta. Another explanation may be that including a random effect of year, a spatial smooth, and a day of year covariate explained much of the same variation as these covariates. However, we do not believe this to be the case because post hoc exploratory analyses demonstrated the same findings even after removing the random effect of year and the spatial smooth parameter. Regardless, our use of a dynamic, spatial model allowed us to capture the variation in the data to, presumably, increase predictive performance and provide a better understanding of the dynamics of distribution and abundance for this species.

The management of unharvested, at-risk animal populations typically focuses on maintaining or restoring critical habitats (Camaclang et al., 2015). These habitat features are often identified through analyses of relationships between the distribution and abundance of focal taxa and various habitat and climate characteristics (Elith & Leathwick, 2009; Waldock et al., 2022). However, there is growing recognition of the importance of incorporating spatial dynamics and spatial relationships when assessing and managing animal populations, as these factors significantly influence ecological processes and species distributions (Beeton et al., 2015; He et al., 2021). In our study, we detected relatively weak

21508925, 2025, 7, Downloaded from https://esajournals.onlinelibrary.wiley.com/doi/10.1002/ecs2.70326, Wiley Online Library on [14/07/2025]. See the Terms and Conditions (https://onlinelibrary.wiley.com/terms-and-conditions) on Wiley Online Library for rules of use; OA articles are governed by the applicable Creative Commons License

TABLE 4 Mean estimates, SD, upper and lower 95% credible intervals, and odds ratios (ORs) or median ORs for random effects for an abundant state transition probabilities for the three-survey dataset (see Appendix S1: Table S3 for the two-survey dataset).

Parameter	Mean	SD	Lower 95%	Upper 95%	OR
Probability of becoming abundant if unoccupied, ρ_1					
Intercept	−4.65	1.46	−8.21	−2.34	
Year random effect (SD)	1.72	1.85	0.45	7.42	3.49
Spatial smooth (min. estimate) (site)	−0.59	1.74	−5.50	1.36	
Spatial smooth (max. estimate) (site)	0.16	0.54	−0.56	1.64	
Spatial random effect (OR only)					1.11
No. days since last survey	−0.03	1.48	−3.07	2.71	0.97
Probability of becoming abundant if occupied, ρ_2					
Intercept	−3.27	0.80	−4.92	−1.77	
Year random effect (SD)	1.54	0.59	0.73	2.99	3.26
Spatial smooth (min. estimate) (site)	−1.08	1.89	−6.21	1.24	
Spatial smooth (max. estimate) (site)	0.28	0.37	−0.10	1.29	
Spatial random effect (OR only)					1.21
No. days since last survey	−0.20	0.31	−0.50	0.75	1.22
Day of the year	−0.37	0.30	−0.91	0.25	0.69
Day of the year^2	0.61	0.32	0.01	1.29	1.84
Bottom depth	0.55	0.17	0.23	0.89	1.74
Tidally connected willow wetland	−1.67	0.74	−3.23	−0.31	0.19
Bay flat	0.11	0.17	−0.22	0.46	1.11
Probability of remaining abundant, ρ_3					
Intercept	−3.33	0.89	−5.18	−1.66	
Year random effect (SD)	1.04	0.47	0.34	2.19	2.64
Spatial smooth (min. estimate) (site)	−0.13	0.62	−1.64	0.80	
Spatial smooth (max. estimate) (site)	0.10	0.30	−0.32	0.92	
Spatial random effect (OR only)					1.06
No. days since last survey	−1.53	0.67	−2.95	−0.34	0.22
Day of the year	0.13	0.59	−1.13	1.23	1.13
Day of the year^2	1.23	0.40	0.45	2.01	3.43
Bottom depth	0.50	0.20	0.13	0.92	1.64
Woody slope unnatural	−2.26	1.01	−4.38	−0.46	0.10
Tidally connected willow wetland	−1.17	0.91	−3.00	0.60	0.31

Note: Transitional probabilities are conditional on the occupancy state during the previous survey.

statistical relationships between tidal stage and a few local (site-level) habitat characteristics and the occupancy state transitions. By contrast, the spatial random effects suggested that the location of a site within the sampling network had a greater influence on the distribution and abundance of Longfin Smelt. This pattern aligns with observations of Delta Smelt in the San Francisco Estuary, where distribution and abundance were weakly correlated with local habitat conditions but exhibited strong spatial structuring that persisted over time (Polansky et al., 2018). The observed spatial effects likely reflect predictable movement patterns of smelt throughout the estuary. Notably, the large spatial effect on the probability of remaining occupied, once a site was occupied, indicated a strong persistent effect associated with specific sites that was unrelated to any of the factors considered in this analysis. This finding suggests that unmeasured or unknown factors may play a significant role in shaping the distribution of Longfin Smelt in the San Francisco Bay-Estuary. Further research is needed to identify and quantify these factors, which could enhance conservation strategies for this and other similarly distributed species.

21508925, 2025, 7, Downloaded from https://esajournals.onlinelibrary.wiley.com/doi/10.1002/ecs2.70326, Wiley Online Library on [14/07/2025]. See the Terms and Conditions (https://onlinelibrary.wiley.com/terms-and-conditions) on Wiley Online Library for rules of use; OA articles are governed by the applicable Creative Commons License

TABLE 5 Mean estimates, SD, upper and lower 95% credible intervals, and odds ratios (ORs) for and detection probability parameters for the three-survey (20-mm, Summer Tow Net [STN], and Fall Midwater Trawl [FMWT]) integrated dataset (see Appendix S1: Figure S3 for the two-survey dataset).

Parameter	Mean	SD	Lower 95%	Upper 95%	OR
Detection probability: p_2					
Intercept[a]	−1.31	0.21	−1.70	−0.91	
STN	−1.56	0.21	−1.97	−1.17	0.21
FMWT	−1.73	0.40	−2.50	−0.90	0.18
Tow volume	0.01	0.08	−0.14	0.16	1.01
Secchi	−2.09	0.23	−2.55	−1.65	0.12
Detection probability, p_{32}					
Intercept[a]	3.47	0.51	2.57	4.55	
STN	−2.23	0.92	−3.98	−0.36	0.11
FMWT	2.46	2.68	−2.37	7.85	11.70
Tow volume	0.63	0.31	−0.03	1.21	1.88
Secchi	−1.77	0.33	−2.44	−1.15	0.17
Detection probability, p_{33}					
Intercept[a]	2.72	0.56	1.68	3.87	
STN	−4.22	0.97	−6.10	−2.24	0.01
FMWT	−3.46	2.58	−8.46	1.58	0.03
Tow volume	0.63	0.32	−0.05	1.22	1.88
Secchi	−3.19	0.40	−3.99	−2.43	0.04

[a]20 mm was the baseline category.

CONCLUSION

While precipitous population declines can—albeit not always—be documented using simple indices, the tools for species recovery will in many cases benefit from a more nuanced understanding of species distribution dynamics. Our spatial dynamic multistate occupancy approach demonstrated that nuanced insights can be obtained from a species absent from 84% of surveys. Although many imperiled species are even rarer, occupancy models can be applied if a sufficient number of sites with replicate surveys have been conducted (MacKenzie et al., 2017). Multistate occupancy abundance models can be applied with a mean true abundance at occupied sites of 3 and at least a modest amount of spatial variation between sites (CV of 0.6); low individual detection probability is sufficient (between 0.1 and 0.3) (Steen et al., 2023). Dynamic occupancy models can be used as long as the cumulative detection probability across replicate visits is not low, even with few sites ($n = 20$) and low initial occupancy probability (0.2) (MacKenzie et al., 2003).

Our spatial dynamic multistate occupancy model results of Longfin Smelt distribution dynamics indicate that woody structure removal may help maintain or promote site-level abundance of this imperiled species. While the Longfin Smelt has become a focus of the data collected by fish monitoring programs in the Bay-Delta, it was not the focus when these programs were established. Thus, surveys—which focus on channels of the upper estuary and the open water bays—have not captured well, for instance, the tidal sloughs and shoals used for rearing by larvae, or the spawning habitats at shallow tidal habitats in the South Bay among, likely, other areas (Grimaldo et al., 2017; Lewis et al., 2020). While our approach utilized a multitude of surveys and a detailed modeling approach, the picture is inevitably incomplete given the absence of surveys in these critical habitats. Still, our analysis approach allowed us to capture various sources of heterogeneity in the data to map spatial predictions of seasonal distribution and abundance patterns for this rare species that can be used to inform policy and management decisions in the Bay-Delta.

ACKNOWLEDGMENTS

This project was funded by the Metropolitan Water District of Southern California, grant no. 187386. Adam Duarte would also like to acknowledge support from the U.S.D.A. Forest Service, Pacific Northwest Research Station. The Oregon Cooperative Fish and

21508925, 2025, 7, Downloaded from https://esajournals.onlinelibrary.wiley.com/doi/10.1002/ecs2.70326, Wiley Online Library on [14/07/2025]. See the Terms and Conditions (https://onlinelibrary.wiley.com/terms-and-conditions) on Wiley Online Library for rules of use; OA articles are governed by the applicable Creative Commons License

Wildlife Research Unit is jointly sponsored by the US Geological Survey, the US Fish and Wildlife Service, the Oregon Department of Fish and Wildlife, Oregon State University, and the Wildlife Management Institute. The use of trade or firm names in this publication is for reader information and does not imply endorsement by the US government of any product or service.

CONFLICT OF INTEREST STATEMENT

The authors declare no conflicts of interest.

DATA AVAILABILITY STATEMENT

Data (Bashevkin et al., 2022) are available on Zenodo: https://doi.org/10.5281/zenodo.6048977.

ORCID

Valerie A. Steen https://orcid.org/0000-0002-1417-8139
Adam Duarte https://orcid.org/0000-0003-0034-1764

REFERENCES

Bain, M. B., N. Haley, D. L. Peterson, K. K. Arend, K. E. Mills, and P. J. Sullivan. 2007. "Recovery of a US Endangered Fish." *PLoS One* 2: e168. https://doi.org/10.1371/journal.pone.0000168.

Bashevkin, S. M., J. W. Gaeta, T. X. Nguyen, L. Mitchell, and S. Khanna. 2022. "'LTMRdata': An R Package to Integrate Data from 9 Fish Surveys in the San Francisco Estuary." v2.2.0. Zenodo. https://doi.org/10.5281/zenodo.6048977.

Beeton, N. J., C. R. McMahon, G. J. Williamson, J. Potts, J. Bloomer, M. N. Bester, L. K. Forbes, and C. N. Johnson. 2015. "Using the Spatial Population Abundance Dynamics Engine for Conservation Management." *Methods in Ecology and Evolution* 6(12): 1407–16. https://doi.org/10.1111/2041-210X.12434.

Camaclang, A. E., M. Maron, T. G. Martin, and H. P. Possingham. 2015. "Current Practices in the Identification of Critical Habitat for Threatened Species." *Conservation Biology* 29(2): 482–492. https://doi.org/10.1111/cobi.12428.

CDFW (California Department of Fish and Wildlife). 2018. "Longfin Smelt." https://wildlife.ca.gov/Conservation/Fishes/Longfin-Smelt.

Clark, J., and S. M. Bashevkin. 2022. "'deltafish': An R Package to Access an Integrated Dataset of Fish Counts and Lengths from the San Francisco Estuary." v0.1.0. Zenodo. https://doi.org/10.5281/zenodo.6484440.

Collier, B. A., J. E. Groce, M. L. Morrison, J. C. Newnam, A. J. Campomizzi, S. L. Farrell, H. A. Mathewson, R. T. Snelgrove, R. J. Carroll, and R. N. Wilkins. 2012. "Predicting Patch Occupancy in Fragmented Landscapes At the Rangewide Scale for an Endangered Species: An Example of an American Warbler." *Diversity and Distributions* 18(2): 158–167. https://doi.org/10.1111/j.1472-4642.2011.00831.x.

Coonan, T. J., C. A. Schwemm, and D. K. Garcelon. 2010. *Decline and Recovery of the Island Fox: A Case Study for Population Recovery*. Cambridge: Cambridge University Press.

de Paula Costa, M. D., R. A. Magris, J. H. Muelbert, J. P. Vieira, J. P. Castello, M. S. Copertino, and H. P. Possingham. 2022. "Spatial Zoning to Conserve Fish Species with Complex Life Cycles in Estuaries." *Ocean and Coastal Management* 221: 106115. https://doi.org/10.1016/j.ocecoaman.2022.106115.

Dellaportas, P., J. J. Forster, and I. Ntzoufras. 2002. "On Bayesian Model and Variable Selection Using MCMC." *Statistics and Computing* 12(1): 27–36.

Dormann, C. F. 2007. "Effects of Incorporating Spatial Autocorrelation into the Analysis of Species Distribution Data." *Global Ecology and Biogeography* 16(2): 129–138. https://doi.org/10.1111/j.1466-8238.2006.00279.x.

Dormann, C. F., J. M. McPherson, M. B. Araújo, R. Bivand, J. Bolliger, G. Carl, R. G. Davies, et al. 2007. "Methods to Account for Spatial Autocorrelation in the Analysis of Species Distributional Data: A Review." *Ecography* 30(5): 609–628. https://doi.org/10.1111/j.2007.0906-7590.05171.x.

Duarte, A., and J. T. Peterson. 2021. "Space-for-Time Is Not Necessarily a Substitution When Monitoring the Distribution of Pelagic Fishes in the San Francisco Bay-Delta." *Ecology and Evolution* 11(23): 16727–44. https://doi.org/10.1002/ece3.8292.

Durso, A. M., J. D. Willson, and C. T. Winne. 2011. "Needles in Haystacks: Estimating Detection Probability and Occupancy of Rare and Cryptic Snakes." *Biological Conservation* 144: 1508–15. https://doi.org/10.1016/j.biocon.2011.01.020.

Elith, J., and J. R. Leathwick. 2009. "Species Distribution Models: Ecological Explanation and Prediction across Space and Time." *Annual Review of Ecology, Evolution, and Systematics* 40(1): 677–697. https://doi.org/10.1146/annurev.ecolsys.110308.120159.

Grimaldo, L., F. Feyrer, J. Burns, and D. Maniscalco. 2017. "Sampling Uncharted Waters: Examining Rearing Habitat of Larval Longfin Smelt (*Spirinchus thaleichthys*) in the Upper San Francisco Estuary." *Estuaries and Coasts* 40(6): 1771–84. https://doi.org/10.1007/s12237-017-0255-9.

Grimaldo, L., J. Burns, R. E. Miller, A. Kalmbach, A. Smith, J. Hassrick, and C. Brennan. 2020. "Forage Fish Larvae Distribution and Habitat Use during Contrasting Years of Low and High Freshwater Flow in the San Francisco Estuary." *San Francisco Estuary and Watershed Science* 18(3):5. https://doi.org/10.15447/sfews.2020v18iss3art5.

Gu, W., and R. K. Swihart. 2004. "Absent or Undetected? Effects of Non-Detection of Species Occurrence on Wildlife–Habitat Models." *Biological Conservation* 116(2): 195–203. https://doi.org/10.1016/S0006-3207(03)00190-3.

Guest, M. A., R. M. Connolly, and N. R. Loneragan. 2003. "Seine Nets and Beam Trawls Compared by Day and Night for Sampling Fish and Crustaceans in Shallow Seagrass Habitat." *Fisheries Research* 64(2–3): 185–196. https://doi.org/10.1016/S0165-7836(03)00109-7.

Guillera-Arroita, G. 2017. "Modelling of Species Distributions, Range Dynamics and Communities under Imperfect Detection: Advances, Challenges and Opportunities." *Ecography* 40(2): 281–295. https://doi.org/10.1111/ecog.02445.

Guisan, A., and W. Thuiller. 2005. "Predicting Species Distribution: Offering More than Simple Habitat Models." *Ecology Letters* 8(9): 993–1009. https://doi.org/10.1111/j.1461-0248.2005.00792.x.

Hammock, B. G., R. Hartman, S. B. Slater, A. Hennessy, and S. J. Teh. 2019. "Tidal Wetlands Associated with Foraging Success

21508925, 2025, 7, Downloaded from https://esajournals.onlinelibrary.wiley.com/doi/10.1002/ecs2.70326, Wiley Online Library on [14/07/2025]. See the Terms and Conditions (https://onlinelibrary.wiley.com/terms-and-conditions) on Wiley Online Library for rules of use; OA articles are governed by the applicable Creative Commons License

of Delta Smelt." *Estuaries and Coasts* 42(3): 857–867. https://doi.org/10.1007/s12237-019-00521-5.

He, P., P. O. Montiglio, M. Somveille, M. Cantor, and D. R. Farine. 2021. "The Role of Habitat Configuration in Shaping Animal Population Processes: A Framework to Generate Quantitative Predictions." *Oecologia* 196(3): 649–665.

Herbold, B., E. Bush, G. Castillo, D. Colombano, R. Hartman, P. Lehman, B. Mahardja, and T. Sommer. 2022. "Climate Change Impacts on San Francisco Estuary Aquatic Ecosystems: A Review." *San Francisco Estuary and Watershed Science* 20(2):1. https://doi.org/10.15447/sfews.2022v20iss2art1.

Hobbs, J., P. B. Moyle, N. Fangue, and R. E. Connon. 2017. "Is Extinction Inevitable for Delta Smelt and Longfin Smelt? An Opinion and Recommendations for Recovery." *San Francisco Estuary and Watershed Science* 15(2):2. https://doi.org/10.15447/sfews.2017v15iss2art2.

Hooten, M. B., and N. T. Hobbs. 2015. "A Guide to Bayesian Model Selection for Ecologists." *Ecological Monographs* 85(1): 3–28. https://doi.org/10.1890/14-0661.1.

Howard, C., P. A. Stephens, J. W. Pearce-Higgins, R. D. Gregory, and S. G. Willis. 2014. "Improving Species Distribution Models: The Value of Data on Abundance." *Methods in Ecology and Evolution* 5(6): 506–513. https://doi.org/10.1111/2041-210X.12184.

Hurlbert, S. H. 1984. "Pseudoreplication and the Design of Ecological Experiments." *Ecological Monographs* 54: 187–211. https://doi.org/10.2307/1942661.

Jeliazkov, A., Y. Gavish, C. J. Marsh, J. Geschke, N. Brummitt, D. Rocchini, P. Haase, W. E. Kunin, and K. Henle. 2022. "Sampling and Modelling Rare Species: Conceptual Guidelines for the Neglected Majority." *Global Change Biology* 28(12): 3754–77. https://doi.org/10.1111/gcb.16114.

Kaartvedt, S., A. Staby, and D. L. Aksnes. 2012. "Efficient Trawl Avoidance by Mesopelagic Fishes Causes Large Underestimation of Their Biomass." *Marine Ecology Progress Series* 456: 1–6. https://doi.org/10.3354/meps09785.

Kellner, K. 2018. "Package 'jagsUI'." https://cran.r-project.org/package=jagsUI.

Kéry, M., and J. A. Royle. 2016. *Applied Hierarchical Modeling in Ecology: Analysis of Distribution, Abundance and Species Richness in R and BUGS: Volume 1: Prelude and Static Models*. Burlington, MA: Academic Press.

Kéry, M., and J. A. Royle. 2020. *Applied Hierarchical Modeling in Ecology: Analysis of Distribution, Abundance and Species Richness in R and BUGS: Volume 2: Dynamic and Advanced Models*. Burlington, MA: Academic Press.

Kéry, M., G. Guillera-Arroita, and J. L. Lahoz-Monfort. 2013. "Analysing and Mapping Species Range Dynamics Using Occupancy Models." *Journal of Biogeography* 40(8): 1463–74. https://doi.org/10.1111/jbi.12087.

Kimmerer, W. J. 2004. "Open Water Processes of the San Francisco Estuary: From Physical Forcing to Biological Responses." *San Francisco Estuary and Watershed Science* 2(1):1. https://doi.org/10.15447/sfews.2004v2iss1art1.

Kimmerer, W. J. 2008. "Losses of Sacramento River Chinook Salmon and Delta Smelt to Entrainment in Water Diversions in the Sacramento–san Joaquin Delta." *San Francisco Estuary and Watershed Science* 6(2):2. https://doi.org/10.15447/sfews.2008v6iss2art2.

Kimmerer, W. J., and J. J. Orsi. 1996. "Changes in the Zooplankton of the San Francisco Bay Estuary since the Introduction of the Clam Potamocorbula Amurensis." In *San Francisco Bay: The Ecosystem*, edited by T.J. Baxter, S.R. Gephard and D.O. Davis, 403–424. San Francisco, CA: Pacific Division, American Association for the Advancement of Science/Pacific Science Center.

Larsen, K., J. H. Petersen, E. Budtz-Jørgensen, and L. Endahl. 2000. "Interpreting Parameters in the Logistic Regression Model with Random Effects." *Biometrics* 56(3): 909–914. https://www.jstor.org/stable/2676942.

Latour, R. J. 2016. "Explaining Patterns of Pelagic Fish Abundance in the Sacramento-San Joaquin Delta." *Estuaries and Coasts* 39: 233–247. https://doi.org/10.1007/s12237-015-9968-9.

Lewis, L. S., M. Willmes, A. Barros, P. K. Crain, and J. A. Hobbs. 2020. "Newly Discovered Spawning and Recruitment of Threatened Longfin Smelt in Restored and Underexplored Tidal Wetlands." *Ecology* 101(1): e02868. https://doi.org/10.1002/ecy.2868.

Linkie, M., Y. Dinata, A. Nugroho, and I. A. Haidir. 2007. "Estimating Occupancy of a Data Deficient Mammalian Species Living in Tropical Rainforests: Sun Bears in the Kerinci Seblat Region, Sumatra." *Biological Conservation* 137: 20–27. https://doi.org/10.1016/j.biocon.2007.01.016.

Lomba, A., L. Pellissier, C. Randin, J. Vicente, F. Moreira, J. Honrado, and A. Guisan. 2010. "Overcoming the Rare Species Modelling Paradox: A Novel Hierarchical Framework Applied to an Iberian Endemic Plant." *Biological Conservation* 143(11): 2647–57. https://doi.org/10.1016/j.biocon.2010.07.007.

Mac Nally, R., J. R. Thomson, W. J. Kimmerer, F. Feyrer, K. B. Newman, A. Sih, W. A. Bennett, et al. 2010. "Analysis of Pelagic Species Decline in the Upper San Francisco Estuary Using Multivariate Autoregressive Modeling (MAR)." *Ecological Applications* 20(5): 1417–30. https://doi.org/10.1890/09-1724.1.

MacKenzie, D. I., J. D. Nichols, J. A. Royle, K. H. Pollock, L. Bailey, and J. E. Hines. 2006. *Occupancy Estimation and Modeling: Inferring Patterns and Dynamics of Species Occurrence*. Burlington, MA: Academic Press.

MacKenzie, D. I., J. D. Nichols, J. A. Royle, K. H. Pollock, L. Bailey, and J. E. Hines. 2017. *Occupancy Estimation and Modeling: Inferring Patterns and Dynamics of Species Occurrence*. Burlington, MA: Academic Press.

MacKenzie, D. I., J. D. Nichols, J. E. Hines, M. G. Knutson, and A. B. Franklin. 2003. "Estimating Site Occupancy, Colonization, and Local Extinction When a Species Is Detected Imperfectly." *Ecology* 84(8): 2200–2207. https://doi.org/10.1890/02-3090.

MacKenzie, D. I., J. D. Nichols, M. E. Seamans, and R. J. Gutiérrez. 2009. "Modeling Species Occurrence Dynamics with Multiple States and Imperfect Detection." *Ecology* 90(3): 823–835. https://doi.org/10.1890/08-0141.1.

Mahardja, B., M. J. Young, B. Schreier, and T. Sommer. 2017. "Understanding Imperfect Detection in a San Francisco Estuary Long-Term Larval and Juvenile Fish Monitoring

21508925, 2025, 7, Downloaded from https://esajournals.onlinelibrary.wiley.com/doi/10.1002/ecs2.70326, Wiley Online Library on [14/07/2025]. See the Terms and Conditions (https://onlinelibrary.wiley.com/terms-and-conditions) on Wiley Online Library for rules of use; OA articles are governed by the applicable Creative Commons License

Programme." *Fisheries Management and Ecology* 24(6): 488–503. https://doi.org/10.1111/fme.12257.

Merz, J. E., P. S. Bergman, J. F. Melgo, and S. Hamilton. 2013. "Longfin Smelt: Spatial Dynamics and Ontogeny in the San Francisco Estuary, California." *California Fish and Game* 99(3): 122–148.

Mitchell, L., K. Newman, and R. Baxter. 2017. "A Covered Cod-End and Tow-Path Evaluation of Midwater Trawl Gear Efficiency for Catching Delta Smelt (*Hypomesus transpacificus*)." *San Francisco Estuary and Watershed Science* 15(4):3.

Mitchell, L., K. Newman, and R. Baxter. 2019. "Estimating the Size Selectivity of Fishing Trawls for a Short-Lived Fish Species." *San Francisco Estuary and Watershed Science* 17(1):5. https://doi.org/10.15447/sfews.2017v15iss4art3.

Moyle, P. B. 2002. *Inland Fishes of California: Revised and Expanded*. Berkeley, CA: University of California Press.

Moyle, P. B., J. V. Katz, and R. M. Quiñones. 2011. "Rapid Decline of California's Native Inland Fishes: A Status Assessment." *Biological Conservation* 144(10): 2414–23. https://doi.org/10.1016/j.biocon.2011.06.002.

Newman, K. B. 2008. "Sample Design-Based Methodology for Estimating Delta Smelt Abundance." *San Francisco Estuary and Watershed Science* 6(3):3. https://doi.org/10.15447/sfews.2008v6iss3art3.

Nobriga, M. L., and J. A. Rosenfield. 2016. "Population Dynamics of an Estuarine Forage Fish: Disaggregating Forces Driving Long-Term Decline of Longfin Smelt in California's San Francisco Estuary." *Transactions of the American Fisheries Society* 145(1): 44–58. https://doi.org/10.1080/00028487.2015.1100136.

Nychka, D., R. Furrer, J. Paige, and S. Sain. 2021. "fields: Tools for Spatial Data." R Package Version 14.1. https://github.com/dnychka/fieldsRPackage.

Pearce, J., and S. Ferrier. 2001. "The Practical Value of Modelling Relative Abundance of Species for Regional Conservation Planning: A Case Study." *Biological Conservation* 98(1): 33–43. https://doi.org/10.1016/S0006-3207(00)00139-7.

Peterson, J. T., and C. P. Paukert. 2009. "Converting Nonstandard Fish Sampling Data to Standardized Data." In *Standard Methods for Sampling North American Freshwater Fishes*, edited by S. A. Bonar, W. A. Hubert, and D. W. Willis, 195–215. Bethesda, MD: American Fisheries Society.

Peterson, J. T., and M. F. Barajas. 2018. "An Evaluation of Three Fish Surveys in the San Francisco Estuary, 1995–2015." *San Francisco Estuary and Watershed Science* 16(4):2. https://doi.org/10.15447/sfews.2018v16iss4art2.

Peterson, J. T., E. McCreless, A. Duarte, P. Wohner, S. Hamilton, J. Medellín-Azuara, and A. Escriva-Bou. 2024. "Prototyping Structured Decision Making for Water Resource Management in the San Francisco Bay-Delta." *Environmental Science and Policy* 157: 103775. https://doi.org/10.1016/j.envsci.2024.103775.

Plummer, M. 2003. "JAGS: A Program for Analysis of Bayesian Graphical Models Using Gibbs Sampling." *Proceedings of the 3rd International Workshop on Distributed Statistical Computing* 124(10): 1–10.

Polansky, L., K. B. Newman, M. L. Nobriga, and L. Mitchell. 2018. "Spatiotemporal Models of an Estuarine Fish Species to Identify Patterns and Factors Impacting their Distribution and Abundance." *Estuaries and Coasts* 41: 572–581. https://doi.org/10.1007/s12237-017-0277-3.

R Core Team. 2023. *R: A Language and Environment for Statistical Computing*. Vienna: R Foundation for Statistical Computing. https://www.R-project.org/.

Rakowitz, G., M. Tušer, M. Říha, T. Jůza, H. Balk, and J. Kubečka. 2012. "Use of High-Frequency Imaging Sonar (DIDSON) to Observe Fish Behaviour Towards a Surface Trawl." *Fisheries Research* 123: 37–48. https://doi.org/10.1016/j.fishres.2011.11.018.

Raudenbush, S. W., and A. S. Bryk. 2002. *Hierarchical Linear Models: Applications and Data Analysis Methods*, Vol. 1. Newbury Park, CA: Sage Publications.

Rosenberg, K. V., J. A. Kennedy, R. Dettmers, R. P. Ford, D. Reynolds, J. D. Alexander, C. J. Beardmore, et al. 2016. "Partners in Flight Landbird Conservation Plan: 2016 Revision for Canada and Continental United States." *Partners in Flight Science Committee* 119: 1–124.

Rosenfield, J. A., and R. D. Baxter. 2007. "Population Dynamics and Distribution Patterns of Longfin Smelt in the San Francisco Estuary." *Transactions of the American Fisheries Society* 136(6): 1577–92. https://doi.org/10.1577/T06-148.1.

SFEI (San Francisco Estuary Institute). 2022. "Delta Aquatic Resource Inventory (DARI), Version 1.1 GIS Data." https://www.sfei.org/data/delta-aquatic-resource-inventory-dari.

SFEI ASC (San Francisco Estuary Institute and Aquatic Science Center). 2017. "Bay Area Aquatic Resource Inventory (BAARI) Version 2.1 GIS Data." http://www.sfei.org/data/baari-version-21-gis-data.

Simonis, J. L., and J. E. Merz. 2019. "Prey Availability, Environmental Constraints, and Aggregation Dictate Population Distribution of an Imperiled Fish." *Ecosphere* 10(3): e02634. https://doi.org/10.1002/ecs2.2634.

Solomon, B. 1998. "Impending Recovery of Kirtland's Warbler: Case Study in the Effectiveness of the Endangered Species Act." *Environmental Management* 22: 9–17. https://doi.org/10.1007/s002679900080.

Sommer, T., and F. Mejia. 2013. "A Place to Call Home: A Synthesis of Delta Smelt Habitat in the Upper San Francisco Estuary." *San Francisco Estuary and Watershed Science* 11(2): 4. https://doi.org/10.15447/sfews.2013v11iss2art4.

Sommer, T., C. Armor, R. Baxter, R. Breuer, L. Brown, M. Chotkowski, S. Culberson, and K. Souza. 2007. "The Collapse of Pelagic Fishes in the Upper San Francisco Estuary: El Colapso de los Peces Pelagicos en la Cabecera del Estuario San Francisco." *Fisheries* 32(6): 270–77. https://doi.org/10.1577/1548-8446(2007)32[270:TCOPFI]2.0.CO;2.

Specht, H. M., H. T. Reich, F. Iannarilli, M. R. Edwards, S. P. Stapleton, M. D. Weegman, M. K. Johnson, B. J. Yohannes, and T. W. Arnold. 2017. "Occupancy Surveys with Conditional Replicates: An Alternative Sampling Design for Rare Species." *Methods in Ecology and Evolution* 8(12): 1725–34. https://doi.org/10.1111/2041-210X.12842.

Steen, V. A., A. Duarte, and J. T. Peterson. 2023. "An Evaluation of Multistate Occupancy Models for Estimating Relative Abundance and Population Trends." *Ecological Modelling* 478: 110303. https://doi.org/10.1016/j.ecolmodel.2023.110303.

Stompe, D. K., P. B. Moyle, A. Kruger, and J. R. Durand. 2020. "Comparing and Integrating Fish Surveys in the San Francisco Estuary: Why Diverse Long-Term Monitoring Programs Are Important." *San Francisco Estuary and Watershed Science* 18(2):4. https://doi.org/10.15447/sfews.2020v18iss2art4.

21508925, 2025, 7, Downloaded from https://esajournals.onlinelibrary.wiley.com/doi/10.1002/ecs2.70326, Wiley Online Library on [14/07/2025]. See the Terms and Conditions (https://onlinelibrary.wiley.com/terms-and-conditions) on Wiley Online Library for rules of use; OA articles are governed by the applicable Creative Commons License

Sweetnam, D., and D. Stevens. 1993. *Report to the Fish and Game Commission: A Status Review of the Delta Smelt (Hypomesus transpacificus) in California. Candidate Species Status Report 93-DS*. Sacramento, CA: California Department of Fish and Game.

Thomson, J. R., W. J. Kimmerer, L. R. Brown, K. B. Newman, R. M. Nally, W. A. Bennett, R. Mac Nally, F. Feyrer, and E. Fleishman. 2010. "Bayesian Change Point Analysis of Abundance Trends for Pelagic Fishes in the Upper San Francisco Estuary." *Ecological Applications* 20(5): 1431–48. https://doi.org/10.1890/09-0998.1.

Tyre, A. J., B. Tenhumberg, S. A. Field, D. Niejalke, K. Parris, and H. P. Possingham. 2003. "Improving Precision and Reducing Bias in Biological Surveys: Estimating False-Negative Error Rates." *Ecological Applications* 13(6): 1790–1801. https://doi.org/10.1890/02-5078.

US EPA (United States Environmental Protection Agency). n.d. "San Francisco Bay Delta Watershed." https://www.epa.gov/sfbay-delta/about-watershed.

USFWS (United States Fish and Wildlife Service). 1996. *Sacramento-San Joaquin Delta Native Fishes Recovery Plan*. Portland, OR: U.S. Fish and Wildlife Service. http://ecos.fws.gov/docs/recovery_plans/1996/961126.pdf.

Waldock, C., R. D. Stuart-Smith, C. Albouy, W. W. Cheung, G. J. Edgar, D. Mouillot, J. Tjiputra, and L. Pellissier. 2022. "A Quantitative Review of Abundance-Based Species Distribution Models." *Ecography* 45(1): e05694. https://doi.org/10.1111/ecog.05694.

SUPPORTING INFORMATION

Additional supporting information can be found online in the Supporting Information section at the end of this article.

How to cite this article: Steen, Valerie A., James T. Peterson, and Adam Duarte. 2025. "Spatially Dynamic Abundance Patterns for a Rare Fish Species." *Ecosphere* 16(7): e70326. https://doi.org/10.1002/ecs2.70326

21508925, 2025, 7, Downloaded from https://esajournals.onlinelibrary.wiley.com/doi/10.1002/ecs2.70326, Wiley Online Library on [14/07/2025]. See the Terms and Conditions (https://onlinelibrary.wiley.com/terms-and-conditions) on Wiley Online Library for rules of use; OA articles are governed by the applicable Creative Commons License